

See discussions, stats, and author profiles for this publication at: <https://www.researchgate.net/publication/7332821>

# Metal-Induced Reductive Ring Opening of 1,2,4,5-Tetrazines: Three Resulting Coordination Alternatives, Including the New Non-Innocent 1,2-Diiminohydrazido(2-) Bridging Ligand System...

ARTICLE *in* INORGANIC CHEMISTRY · FEBRUARY 2006

Impact Factor: 4.76 · DOI: 10.1021/ic051532p · Source: PubMed

CITATIONS

42

READS

124

8 AUTHORS, INCLUDING:



**Somnath Maji**

Indian Institute of Technology Hyderabad

37 PUBLICATIONS 587 CITATIONS

SEE PROFILE



**Srikanta Patra**

Indian Institute of Technology Bhubaneswar

32 PUBLICATIONS 777 CITATIONS

SEE PROFILE



**Mohammad Mobin Shaikh**

Indian Institute of Technology Indore

325 PUBLICATIONS 5,267 CITATIONS

SEE PROFILE



**Vedavati G Puranik**

CSIR - National Chemical Laboratory, Pune

224 PUBLICATIONS 2,831 CITATIONS

SEE PROFILE

# Metal-Induced Reductive Ring Opening of 1,2,4,5-Tetrazines: Three Resulting Coordination Alternatives, Including the New Non-Innocent 1,2-Diiminohydrazido(2–) Bridging Ligand System

Somnath Maji,<sup>†</sup> Biprajit Sarkar,<sup>‡</sup> Srikanta Patra,<sup>†</sup> Jan Fiedler,<sup>§</sup> Shaikh M. Mobin,<sup>†</sup> Vedavati G. Puranik,<sup>||</sup> Wolfgang Kaim,<sup>\*,‡</sup> and Goutam Kumar Lahiri<sup>\*,†</sup>

Contribution from the Department of Chemistry, Indian Institute of Technology–Bombay, Powai, Mumbai-400076, India, Institut für Anorganische Chemie, Universität Stuttgart, Pfaffenwaldring 55, D-70550 Stuttgart, Germany, J. Heyrovský Institute of Physical Chemistry, Academy of Sciences of the Czech Republic, Dolejškova 3, CZ-18223 Prague, Czech Republic, and Center for Materials Characterization, National Chemical Laboratory, Pune, Maharashtra-411008, India

Received September 8, 2005

Reaction of 3,6-diaryl-1,2,4,5-tetrazines (aryl = R = phenyl, 2-furyl or 2-thienyl) with 2 equiv of  $\text{Ru}(\text{acac})_2(\text{CH}_3\text{CN})_2$  results in reductive tetrazine ring opening to yield diruthenium complexes  $[(\text{acac})_2\text{Ru}^{\text{III}}(\text{dih-R}^{2-})\text{Ru}^{\text{III}}(\text{acac})_2]$  bridged by the new 1,2-diiminohydrazido(2–) ( $\text{dih-R}^{2-} = \text{HNC(R)NNC(R)NH}^{2-}$ ) ligands. *rac/meso* diastereoisomers could be detected and separated for the compounds with R = phenyl and 2-thienyl, all species are diamagnetic and were characterized by  $^1\text{H}$  NMR spectroscopy. Crystal structure determination of the *meso* isomers with R = phenyl and 2-thienyl confirmed the 1,2-diiminohydrazido formulation through long N–N ( $\approx 1.40$  Å) and short C=N(H) bonds ( $\approx 1.31$  Å), implying two bridged ruthenium(III) centers at about 4.765 Å distance with strong antiferromagnetic coupling. The complexes undergo two reversible and well-separated one-electron reduction and oxidation processes, respectively. EPR Spectroscopy of the paramagnetic intermediates with comproportionation constants  $K_c > 10^{12}$  and UV–vis–NIR spectroelectrochemistry were used to identify the accessible redox states as  $[(\text{acac})_2\text{Ru}^{\text{II}}(\text{dih-R}^{2-})\text{Ru}^{\text{II}}(\text{acac})_2]^{2-}$ ,  $[(\text{acac})_2\text{Ru}^{\text{II}}(\text{dih-R}^{\bullet-})\text{Ru}^{\text{II}}(\text{acac})_2]^-$ ,  $[(\text{acac})_2\text{Ru}^{\text{III}}(\text{dih-R}^{2-})\text{Ru}^{\text{III}}(\text{acac})_2]$ ,  $[(\text{acac})_2\text{Ru}^{\text{III}}(\text{dih-R}^{\bullet-})\text{Ru}^{\text{III}}(\text{acac})_2]^+$ , and  $[(\text{acac})_2\text{Ru}^{\text{III}}(\text{dih-R})\text{Ru}^{\text{III}}(\text{acac})_2]^{2+}$ . While the UV–vis–NIR spectroscopic response of  $[(\text{acac})_2\text{Ru}(\text{dih-R})\text{Ru}(\text{acac})_2]^{0/-2-}$  is very similar to that of  $[(\text{bpy})_2\text{Ru}(\text{adc-R})\text{Ru}(\text{bpy})_2]^{4+/3+/2+}$ ,  $\text{adc-R}^{2-} = 1,2$ -diacylhydrazido(2–), the EPR result indicating ligand-centered spin for  $[(\text{acac})_2\text{Ru}^{\text{II}}(\text{dih-R}^{\bullet-})\text{Ru}^{\text{II}}(\text{acac})_2]^-$  despite deceptive NIR absorptions around 1400 nm reveals distinct differences in the electronic structures.

## Introduction

“Non-innocent” ligands<sup>1a–c</sup> which are redox active and thus do not occur commonly in only one oxidation state are attractive components of functional materials where their

charge-transfer, electron-transfer, and spin-carrier properties in combination with coordinated metals or other organic molecules can be used.<sup>1</sup> However, new metal binding or even metal–metal bridging redox systems have become rare,<sup>2</sup> especially in the area of small molecules which are expected to exert the strongest effects at the metal–ligand interface.

1,2,4,5-Tetrazine and their substituted forms have been established during the past two decades as fairly stable acceptor ligands<sup>3</sup> which do not readily decompose in their coordination compounds, e.g., through photolysis. Nonethe-

\* To whom correspondence should be addressed. E-mail: kaim@iac.uni-stuttgart.de.

<sup>†</sup> Indian Institute of Technology–Bombay.

<sup>‡</sup> Institut für Anorganische Chemie.

<sup>§</sup> J. Heyrovský Institute.

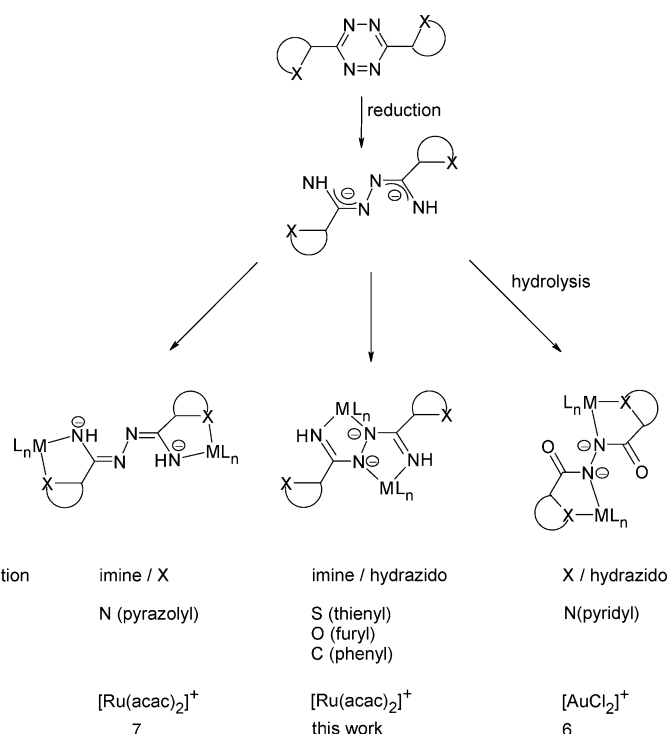
<sup>||</sup> National Chemical Laboratory.

- (1) (a) Jørgensen, C. K. *Oxidation Numbers and Oxidation States*; Springer: Berlin, 1969; p 213. (b) Ward, M. D.; McCleverty, J. A. *J. Chem. Soc., Dalton Trans.* **2002**, 275. (c) Herebian, D.; Bothe, E.; Bill, E.; Weyhermüller, T.; Wieghardt, K. *J. Am. Chem. Soc.* **2001**, *123*, 10012. (d) Oh, M.; Carpenter, G. B.; Sweigart, D. A. *Acc. Chem. Res.* **2004**, *37*, 1. (e) Fourmigué, M. *Acc. Chem. Res.* **2004**, *37*, 179. (f) Drain, C. M.; Hupp, J. T.; Suslick, K. S.; Wasielewski, M. R.; Chen, X. *J. Porphyrins Phthalocyanines* **2002**, *6*, 243.

- (2) (a) Ghuman, S.; Sarkar, B.; Patra, S.; van Slageren, J.; Fiedler, J.; Kaim, W.; Lahiri, G. K. *Inorg. Chem.* **2005**, *45*, 3210. (b) Kar, S.; Sarkar, B.; Ghuman, S.; Janardanan, D.; van Slageren, J.; Fiedler, J.; Puranik, V. G.; Sunoj, R. B.; Kaim, W.; Lahiri, G. K. *Chem. Eur. J.* **2005**, *11*, 4901.

- (3) Kaim, W. *Coord. Chem. Rev.* **2002**, *230*, 127.

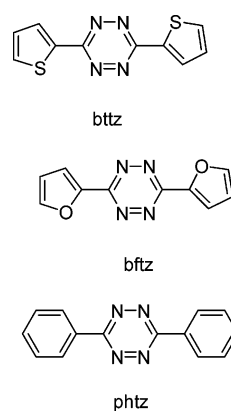
Scheme 1



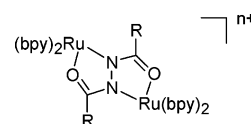
less, despite the formal Hückel aromaticity, the presence of four electronegative nitrogen atoms within a six-membered ring makes 1,2,4,5-tetrazines so electron deficient that facile one-electron reduction to radical intermediates and, at significantly more negative potentials, to two-electron reduced (and thus re-oxidizable) “dihydro” forms can take place.<sup>3,4</sup> Although the two-electron reduction was frequently observed to occur irreversibly,<sup>3</sup> no detailed studies of the follow-up products have been reported so far. Two-electron reduction can involve added charges in the 1,4- or 1,2-position, the latter, higher-energy alternative causing the weakening of one N–N bond. Further reduction of 1,2-dihydro-1,2,4,5-tetrazine should then result in N–N bond cleavage; the acyclic six-atom product can be described as an N,N'-coupled bis-amidinato or as a 1,2-diiminohydrazido(2-) system capable of various metal binding opportunities if one includes potentially coordinating C substituents (Scheme 1).

In fact, a report by Bu and co-workers has recently described that copper-induced (reductive) cleavage of 3,6-bis(2-pyridyl)-1,2,4,5-tetrazine (bptz) can lead to tetranuclear metal complexes with N,N'-bis(α-picolinoyl)hydrazido(2-) bridges;<sup>5a</sup> a 1,3,4-oxadiazole intermediate was proposed.<sup>5</sup> Subsequently, the use of chlorogold(III) compounds was shown to effect a related tetrazine ring cleavage of bptz; however, the final product following imine hydrolysis contained Au<sup>III</sup> bound by the basic 2-pyridyl and hydrazido

Scheme 2



Scheme 3



N atoms (Scheme 1, lower right).<sup>6</sup> In a different kind of reaction, the combination of Ru(acac)<sub>2</sub>(CH<sub>3</sub>CN)<sub>2</sub>, acac<sup>-</sup> = acetylacetonato = 2,4-pentanedionato, with 3,6-bis(3,5-dimethylpyrazolyl)-1,2,4,5-tetrazine produced another coordination mode, involving the pyrazolyl N and the negatively charged NH functions in a ketazine situation of the backbone (Scheme 1, lower left), i.e., leaving the N–N-bonded nitrogen centers uncoordinated.<sup>7</sup>

Using the three differently substituted derivatives 3,6-diphenyl-1,2,4,5-tetrazine (phtz), 3,6-bis(2-furyl)-1,2,4,5-

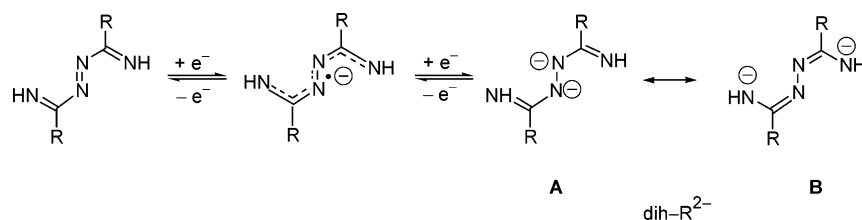
(4) Sauer, J. In *Comprehensive Heterocyclic Chemistry II*; Katritzky, A. R., Rees, C. W., Scriber, E. F. V., Eds; Elsevier Science Ltd.: Oxford, 1996; Vol. 6, p 901.

(5) (a) Bu, X. H.; Liu, H.; Du, M.; Zhang, L.; Guo, Y.-M.; Shionoya, M.; Ribas, J. *Inorg. Chem.* **2002**, *41*, 1855 and 5634. (b) See also Wignacourt, J. P.; Sueur, S.; Lagrenée, M. *Acta Crystallogr., Sect. C* **1990**, *46*, 394. (c) Lagrenée, M.; Sueur, S.; Wignacourt, J. P. *Acta Crystallogr., Sect. C* **1991**, *47*, 1158.

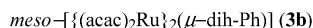
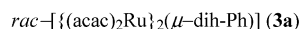
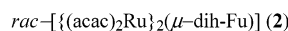
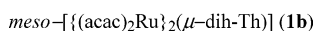
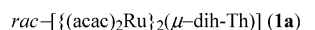
(6) Dogan, A.; Schwederski, B.; Schleid, Th.; Lissner, F.; Fiedler, J.; Kaim, W. *Inorg. Chem. Commun.* **2004**, *7*, 220.

(7) Patra, S.; Miller, T. A.; Sarkar, B.; Niemeyer, M.; Ward, M. D.; Lahiri, G. K. *Inorg. Chem.* **2003**, *42*, 4707.

## Scheme 4



## Scheme 5



tetrazine (bftz), and 3,6-bis(2-thienyl)-1,2,4,5-tetrazine (bttz) (Scheme 2), we can show in this work that non-coordinating (phtz) or poorly metal binding substituents in the 3,6 positions of tetrazines (bftz, bttz) result in a third coordination alternative (Scheme 1, center), involving the four N atoms of the original tetrazine in the form of imino  $\pi$ -acceptor and hydrazido(2-)  $\pi$ -donor centers.

The resulting rigid arrangement with edge-sharing five-membered chelate rings ("S frame configuration") is known to bring the coordinated metals together at a rather close distance of less than 5 Å with several possibilities of  $\pi$ -electron delocalization.<sup>8–10</sup> The related 1,2-diacylhydrazido-(2-) ligands were previously shown to be oxidized to stable radical ion complexes<sup>8</sup> and to stabilize mixed-valent intermediates (Scheme 3).<sup>9</sup>

The replacement of acyl by the much better metal-binding imino functions can be expected to result in a significantly different situation, both energetically and with respect to the electronic structures. Herein, we describe the rather general applicability of the reductive ring-opening reactions of diaryl-substituted 1,2,4,5-tetrazines (Scheme 1) and the properties of the resulting new kinds of dinuclear complexes with [Ru-(acac)<sub>2</sub>]. Particular emphasis is given to the accessible stable redox states (two one-electron reductions and oxidations, respectively) which could be characterized by EPR and UV–vis–NIR spectroelectrochemistry.

## Results and Discussion

**Synthesis, Structure, and Isomerism.** All three substituted tetrazines, bttz, bftz, and phtz, react in the same way with 2 equiv of Ru(acac)<sub>2</sub>(CH<sub>3</sub>CN)<sub>2</sub>. This result already suggests that the substituents are not coordinating, even in the case of bttz with the 2-thienyl groups positioned in a suitable position for metal chelation.<sup>11</sup> According to chro-

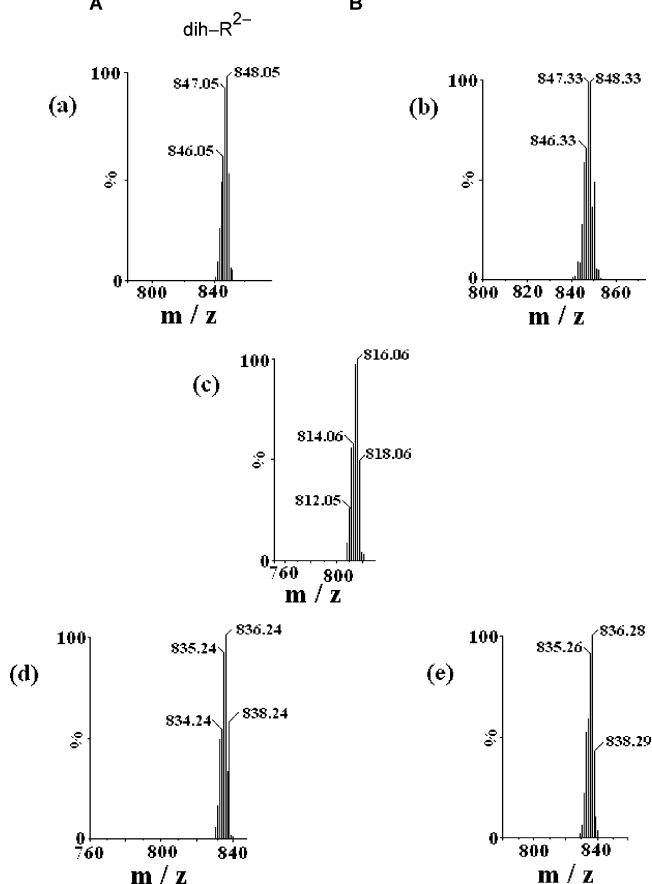


**Figure 1.** ESI-MS spectra of (a) **1a**, (b) **1b**, (c) **2**, (d) **3a**, and (e) **3b** in CH<sub>2</sub>Cl<sub>2</sub>.

matographic separation and <sup>1</sup>H NMR characterization (cf. below), the diamagnetic products were formed as mixtures of two isomers, **1a** and **1b** from bttz and **3a** and **3b** from phtz (see Scheme 5 and Experimental Section); the bftz precursor yielded almost exclusively one isomer, compound **2**. Mass spectroscopy (Figure 1) showed a composition involving two Ru(acac)<sub>2</sub> complex fragments and a formally dehydrogenated, i.e., reduced, ligand which is also confirmed by additional D-exchangeable <sup>1</sup>H NMR signals at low field. In agreement with previous reports on similar  $\beta$ -diketonato–ruthenium complexes<sup>12</sup> rather narrow bands were found at about 3340 cm<sup>−1</sup> for the N–H stretching vibrations.

The crystallization of isomers **1b** and **3b** (Tables 1 and 2 and Figures 2 and 3) allowed for X-ray structure analysis which showed that the tetrazine ring has been opened during the reaction and that only the four former tetrazine N atoms, but not the substituents, participate in metal coordination. While the resulting structure with two nearly coplanar edge-sharing five-membered chelate rings involves a new bis-

(8) Moscherosch, M.; Field, J. S.; Kaim, W.; Kohlmann, S.; Krejci, M. *J. Chem. Soc., Dalton Trans.* **1993**, 211.

(9) Kasack, V.; Kaim, W.; Binder, H.; Jordanov, J.; Roth, E. *Inorg. Chem.* **1995**, 34, 1924.

(10) Kaim, W. *Coord. Chem. Rev.* **2001**, 219–221, 463.

(11) Sarkar, B.; Kaim, W.; Klein, A.; Schwederski, B.; Fiedler, J.; Duboc-Toia, C.; Lahiri, G. K. *Inorg. Chem.* **2003**, 42, 6172.

(12) Hashimoto, T.; Hara, S.; Shiraishi, Y.; Yamauchi, M.; Natarajan, K.; Shimizu, K. *Inorg. Chim. Acta* **2005**, 358, 2207.

**Table 1.** Crystallographic Data for **1b**·0.5H<sub>2</sub>O and **3b**

	<b>1b</b> ·0.5H <sub>2</sub> O	<b>3b</b>
formula	C <sub>30</sub> H <sub>37</sub> N <sub>4</sub> O <sub>8.50</sub> Ru <sub>2</sub> S <sub>2</sub>	C <sub>34</sub> H <sub>40</sub> N <sub>4</sub> O <sub>8</sub> Ru <sub>2</sub>
fw	855.90	834.84
cryst syst	monoclinic	monoclinic
space group	<i>P</i> 2 <sub>1</sub> / <i>c</i>	<i>C</i> 2/ <i>c</i>
<i>T</i> (K)	293(2)	293(2)
<i>λ</i> (Å)	0.71073	0.71073
<i>a</i> (Å)	11.8089(9)	25.225(2)
<i>b</i> (Å)	17.448(1)	10.2960(4)
<i>c</i> (Å)	18.646(2)	15.9520(19)
<i>β</i> (deg)	95.645(2)	122.897(8)
<i>V</i> (Å <sup>3</sup> )	3823.3(5)	3478.7(5)
cryst size (mm <sup>3</sup> )	0.25 × 0.09 × 0.06	0.30 × 0.25 × 0.20
<i>d</i> <sub>calcd</sub> (g cm <sup>-3</sup> )	1.487	1.594
<i>Z</i>	4	4
<i>μ</i> (mm <sup>-1</sup> )	0.949	0.924
<i>F</i> (000)	1732	1696
2 $\theta$ range (deg)	4.18–50.00	3.84–50.00
no. of reflns collected	19 197	3183
no. of ind reflns	6710 [ <i>R</i> (int) = 0.0710]	3059 [ <i>R</i> (int) = 0.0255]
no. of data/restraints/params	6710/20/436	3059/0/221
GOF, <i>F</i> <sup>2</sup>	0.971	1.030
<i>R</i> <sub>1</sub> , <i>wR</i> <sub>2</sub> [ <i>I</i> > 2 $\sigma$ ( <i>I</i> )]	0.0583, 0.1276	0.0445, 0.0882
<i>R</i> <sub>1</sub> , <i>wR</i> <sub>2</sub> (all data)	0.1114, 0.1491	0.1054, 0.1039
largest diff. peak/hole, (e Å <sup>-3</sup> )	0.925/–0.482	0.530/–0.869

**Table 2.** Selected Bond Distances (Å) and Bond Angles (deg) for **1b** and **3b**

	distances			angles <sup>b</sup>	
	<b>1b</b>	<b>3b</b>		<b>1b</b>	<b>3b</b>
Ru1–N1	1.948(5)	1.927(5)	N1–Ru1–N3 <sup>a</sup>	76.6(2)	77.01(18)
Ru1–N3 <sup>a</sup>	2.020(5)	2.012(4)	N1–Ru1–O1	90.5(2)	90.67(18)
Ru1–O1	2.001(4)	2.010(4)	N1–Ru1–O2	95.5(2)	93.90(17)
Ru1–O2	2.038(4)	2.058(4)	N1–Ru1–O3	179.2(2)	176.47(19)
Ru1–O3	2.062(5)	2.065(4)	N1–Ru1–O4	90.7(2)	93.14(17)
Ru1–O4	2.025(5)	2.014(4)	N3 <sup>a</sup> –Ru1–O1	87.1(2)	84.62(17)
Ru2–N2	2.007(5)		N3 <sup>a</sup> –Ru1–O2	172.1(2)	170.42(16)
Ru2–N4	1.951(5)		N3 <sup>a</sup> –Ru1–O3	103.8(2)	103.90(16)
Ru2–O5	1.990(5)		N3 <sup>a</sup> –Ru1–O4	93.7(2)	96.60(17)
Ru2–O6	2.066(5)		N2–Ru2–N4	76.9(2)	
Ru2–O7	2.057(5)		N2–Ru2–O5	90.6(2)	
Ru2–O8	2.019(5)		N2–Ru2–O6	171.5(2)	
N1–C11	1.314(8)	1.318(6)	N2–Ru2–O7	102.2(2)	
N2–C11	1.336(7)	1.334(7)	N2–Ru2–O8	91.2(2)	
N2–N3 <sup>a</sup>	1.397(7)	1.407(8)	N4–Ru2–O5	93.2(2)	
N3–C16	1.342(7)		N4–Ru2–O6	94.6(2)	
N4–C16	1.296(8)		N4–Ru2–O7	176.5(2)	
Ru–Ru	4.769	4.766	N4–Ru2–O8	88.0(2)	

<sup>a</sup> N(2') for **3b**. <sup>b</sup> Angles O–Ru–O 84–93° (cis) and 176–179° (trans).

chelate ligand system, related arrangements have been described before for mixed bis(N,O-donor) ligands derived from azodicarbonyl compounds or from their reduced forms, the diacylhydrazido(2–) ligands.<sup>8,9</sup> The edge-sharing of two five-membered chelate rings involves an “S-frame” structure with the ligand in *s*-trans/*E*/*s*-trans conformation and typically short metal–metal distances of *d* < 5 Å.<sup>8–10</sup> Accordingly, the present two examples **1b** and **3b** have *d*(Ru–Ru) = 4.77 Å.

The dimensions within the new bridging ligand system are revealing: The central N–N bonds are rather long in both cases at about 1.40 Å, close to the expected value for a single bond.<sup>13a</sup> The terminal C=N bonds, on the other hand, in which the N atoms bind the added hydrogen atoms, are

short with average values of about 1.31 Å which suggests a double bond.<sup>13b</sup> Together with the ca. 1.34 Å for the “inner C–N” bonds this result points to alternative **A** in Scheme 4 for the then-dianionic bridging ligands, thus best formulated as C-substituted 1,2-diiminohydrazido(2–) ligands, diH-R<sup>2–</sup> (R = Th = 2-thienyl, R = Fu = 2-furyl, R = Ph = phenyl).

Obviously, the reactions between two ruthenium(II) precursor complexes and the tetrazines have involved extensive electron transfer (4e<sup>–</sup>) accompanied by double protonation, leading to ring-opened, four-electron reduction products of the tetrazine and, in turn, to one-electron oxidation at the metal centers.<sup>14</sup>

Considering the established<sup>15,16</sup> preference for the [Ru(acac)<sub>2</sub>]<sup>n+</sup> complex fragment to adopt the *n* = 1 state with

(13) (a) Huheey, J. E.; Keiter, E. A.; Keiter, R. L. *Inorganic Chemistry*, 4th ed.; HarperCollins: New York, 1993; p A–31. (b) Shriver, D. F.; Atkins P. W.; Langford, C. H. *Inorganic Chemistry*; Oxford University Press: Oxford, 1990; p 69.

(14) The formation of additional ruthenium(III) is evident from Ru(acac)<sub>3</sub> identified as byproduct (see Experimental Section).



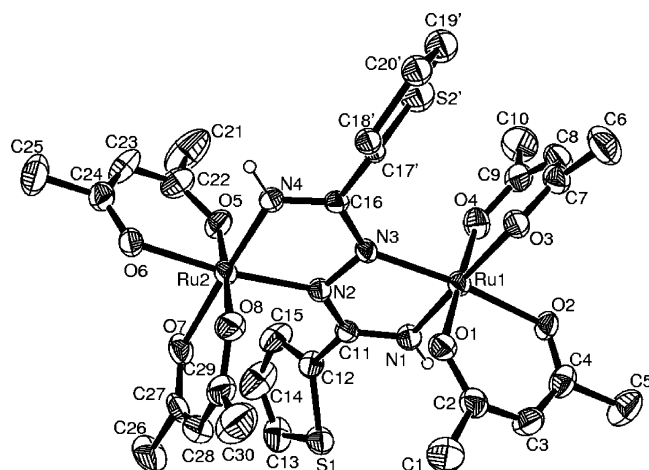


**Figure 2.** ORTEP diagram of **1b**. Ellipsoids are drawn at 30% probability. Hydrogen atoms with the exception of N–H have been omitted for clarity. Only one kind of the disordered thiophene rings is shown.

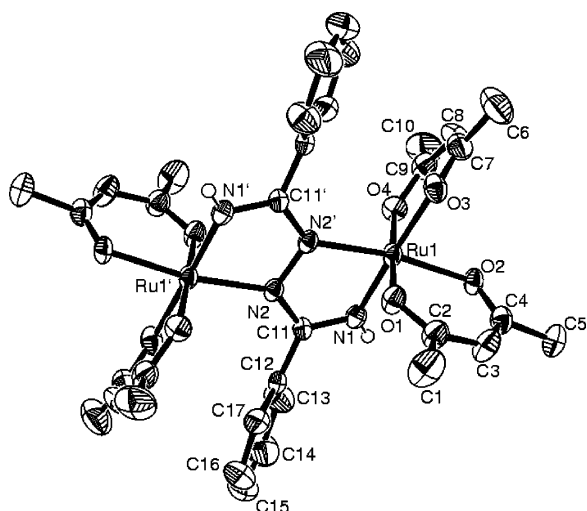


**Figure 3.** ORTEP diagram of **3b**. Ellipsoids are drawn at 50% probability level. Hydrogen atoms with the exception of N–H have been omitted for clarity.

ruthenium(III) configuration, this result is not too surprising; however, the resulting diamagnetism of the complexes ( $\mu$ -dih- $R^{2-}$ )[ $Ru^{III}(\text{acac})_2$ ] $_2$  must then be a consequence of strong ligand-enhanced antiferromagnetic spin–spin coupling. Not only the unusually short metal–metal distances for molecule-bridged dinuclear species but also the electronic mediator effects of the unsaturated and, as we shall see later, non-innocent ligands di- $R^{2-}$  are held responsible for the observed strong spin–spin interaction.

The Ru–N distances differ consistently: At about 2.01 Å, the  $Ru^{III}$ –N(hydrazido) bonds are distinctly longer than the  $Ru^{III}$ –N(imine) bonds at about 1.93 Å. The negative charge localized on the hydrazido N atoms according to resonance form **A** of Scheme 4 is held responsible for this difference. The remaining structural features of compounds

**1b** and **3b** are unremarkable, the aryl substituents are considerably twisted with respect to the central bis-chelate ring plane.

In contrast to recently reported metal-induced ring-opening reactions of tetrazines (Scheme 1),<sup>5–7</sup> the present examples do not make use of the C substituents but rely wholly on the donor set provided originally by the tetrazine ring.

Even symmetrically dinuclear complexes of the described kind can exist as isomers due to the tris-chelate coordination at the metals.<sup>17</sup> In structurally related cases such as  $\{(\mu\text{-abpy})\text{-}[Ru(\text{bpy})_2]_2\}^{4+}$ , the meso and rac isomers could be separated and identified on the basis of NMR spectroscopy,<sup>18</sup> the recently obtained analogues  $(\mu\text{-abpy})[Ru(\text{acac})_2]_2$  could even be crystallized in both forms.<sup>19</sup> The two crystallized compounds **1b** and **3b** in the present case contain meso-configured molecules (Figures 2 and 3); the rac forms are distinguished from the meso isomers mainly by a much larger difference ( $\Delta$ ) between the CH resonances of the  $\text{acac}^-$  coligands ( $\Delta_{\text{meso}} = 0.2$  ppm vs  $\Delta_{\text{rac}} = 0.7$  ppm, see Figure 4 and Experimental Section). According to this criterion, the isolated form **2** from the reaction with bftz is the rac isomer because it has  $\Delta = 0.68$  ppm, Scheme 5 summarizes the assignments.

The other  $^1\text{H}$  NMR resonances, the redox potentials (Table 3) and the absorption spectra (Table 5) show very little differences between rac and meso isomers, which is not unexpected.<sup>17–20</sup>

**Redox Activity of the New Complexes.** The potential redox reactivity of the complex fragments  $[Ru(\text{acac})_2]^{n+}$ ,  $n = 0, 1$ , or  $2$ ,<sup>15,16</sup> and of the new bis-chelate ligand according to Scheme 4 invited electrochemical and spectroelectrochemical studies. To identify the proper oxidation state distribution a combination of UV–vis–NIR absorption spectroscopy and EPR was chosen.

All five isolated complexes undergo two one-electron reductions and two one-electron oxidations in the well-accessible potential region of acetonitrile (Figure 5, Table 3). The processes are reversible as confirmed by spectroelectrochemistry (cf. below), except for the second reductions, **3a** $^{(-)} \rightarrow (-2-)$  and **3b** $^{(-)} \rightarrow (-2-)$ . The results from Table 3 show wide separations between the four waves, leading to very large comproportionation constants  $K_c > 10^{12}$  for the odd-electron intermediates (monoanions or monocations) which may involve radical ligands or mixed-valent metal configurations<sup>9</sup> [ $RT \ln K_c = nF(\Delta E)$ ]. There is relatively little variation between the compounds; all potentials are shifted to slightly more negative values when going from the thienyl via the furyl to the phenyl-substituted systems which thus are the easiest to oxidize and the most difficult to reduce.

The paramagnetic intermediates generated electrochemically from the five neutral complexes through oxidation or

- (15) Patra, S.; Sarkar, B.; Mobin, S. M.; Kaim, W.; Lahiri, G. K. *Inorg. Chem.* **2003**, *42*, 6469.  
 (16) Kar, S.; Sarkar, B.; Ghumaan, S.; Roy, D.; Urbanos, F. A.; Fiedler, J.; Sunoj, R. B.; Jimenez-Aparicio, R.; Kaim, W.; Lahiri, G. K. *Inorg. Chem.* **2005**, *44*, 8715.

- (17) Ernst, S.; Kasack, V.; Kaim, W. *Inorg. Chem.* **1988**, *27*, 1146.  
 (18) Kelso, L. S.; Reitsma, D. A.; Keene, F. R. *Inorg. Chem.* **1996**, *35*, 5144.  
 (19) Sarkar, B.; Patra, S.; Fiedler, J.; Sunoj, R.; Janardanan, D.; Mobin, S. M.; Niemeyer, N.; Lahiri, G. K.; Kaim, W. *Angew. Chem.*, **2005**, *117*, 5800; *Angew. Chem., Int. Ed.* **2005**, *44*, 5655.  
 (20) Heilmann, M.; Frantz, S.; Kaim, W.; Fiedler, J.; Duboc, C. *Inorg. Chim. Acta*, in print (web released; DOI: 10.1016/j.ica.2005.04.044).

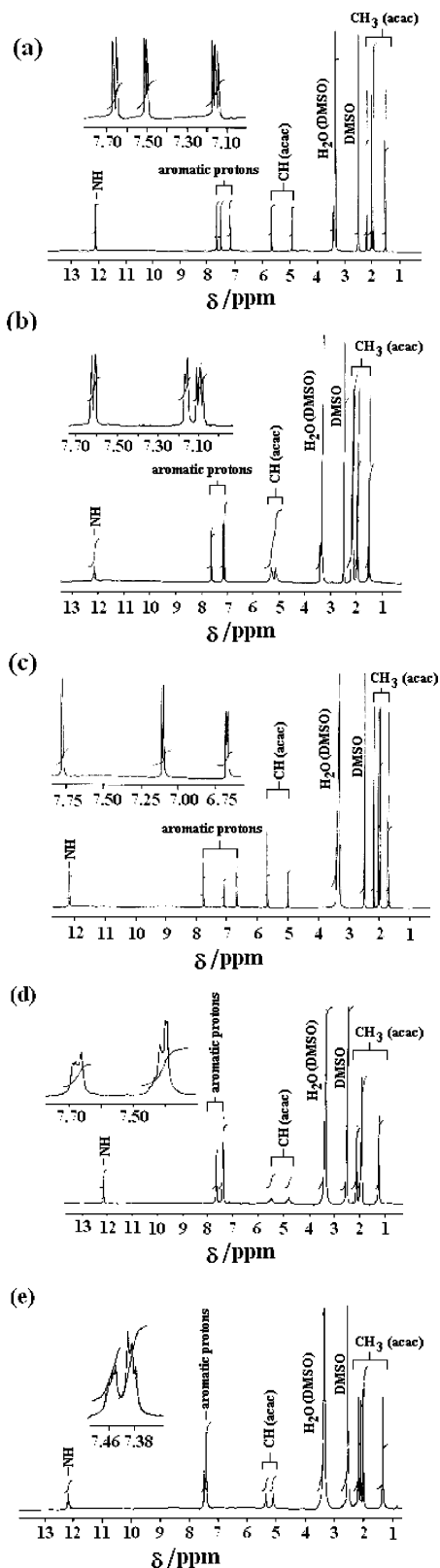


**Figure 4.**  $^1\text{H}$  NMR spectra of (a) **1a**, (b) **1b**, (c) **2**, (d) **3a**, and (e) **3b** in  $(\text{CD}_3)_2\text{SO}$ .

reduction show very similar EPR behavior (Figure 6, Table 4). Oxidation produces signals in glassy frozen solutions which are typical for ruthenium(III),<sup>15,16</sup> i.e., rhombic  $g$  component splitting with  $g > 2$ . Reduction, on the other hand, yields only unresolved signals at isotropic  $g$  values

slightly lower than 2, as is typical for mononuclear and dinuclear radical complexes containing ruthenium(II).<sup>21</sup> Starting from a  $(\text{dih-R}^{2-})(\text{Ru}^{\text{III}})_2$  situation, we conclude from EPR that reduction produces  $(\text{dih-R}^{\bullet-})(\text{Ru}^{\text{II}})_2$  instead of the mixed-valent  $(\text{dih-R}^{2-})\text{Ru}^{\text{II}}\text{Ru}^{\text{III}}$ , despite an intense near-infrared absorption (cf. below). This interpretation implies that the *reduction of the complex* involves an *oxidation of the bridging ligand* with intramolecular electron transfer compensating for the seemingly paradoxical effect. Similar phenomena have been observed before in dioxolene/metal and TCNX/metal chemistry.<sup>22,23</sup> On the other hand, one-electron oxidation leads to metal-centered spin, either in a mixed-valent  $(\text{dih-R}^{2-})\text{Ru}^{\text{III}}\text{Ru}^{\text{IV}}$  situation or in the three-spin system  $\text{Ru}^{\text{III}}(\text{dih-R}^{\bullet-})\text{Ru}^{\text{III}}$  with dominant antiferromagnetic coupling between the radical ligand and one of the two ruthenium(III) centers.<sup>24</sup>

Spectroelectrochemistry in the UV–vis–NIR regions using an optically transparent thin-layer electrode (OTTLE) cell<sup>25</sup> (Figure 7, Table 5) was used to further analyze the oxidation state situation, to elucidate the electronic structures of even-electron systems, and to determine the nature of low-lying excited states.

The neutral products  $(\mu\text{-dih-R})[\text{Ru}(\text{acac})_2]_2$  from the tetrazine ring-opening reactions exhibit intense long-wavelength bands around 730 nm which are attributed to ligand-to-metal charge-transfer transitions from the electron-rich bridges to the two ruthenium(III) centers each.<sup>26</sup> On oxidation, this band is decreased in intensity, yet the position remains almost unchanged; an absorption in the near-infrared, as would be expected<sup>16</sup> for a mixed-valent situation  $(\text{dih-R}^{2-})\text{Ru}^{\text{III}}\text{Ru}^{\text{IV}}$ , was not observed. This result suggests the formulation  $\text{Ru}^{\text{III}}\text{-(dih-R}^{\bullet-})\text{Ru}^{\text{III}}$  for the monocation, i.e., an oxidation of the bridging ligand instead of the metal. The second oxidation causes the long-wavelength band to increase considerably and shift slightly to lower energies; a charge-transfer transition, either MLCT (metal-to-ligand charge transfer) for a formulation  $(\text{dih-R}^{\circ})\text{Ru}^{\text{III}}\text{Ru}^{\text{III}}$  or LMCT in a situation  $(\text{dih-R}^{2-})\text{Ru}^{\text{IV}}\text{Ru}^{\text{IV}}$  can be considered. In the absence of further information, this question must remain open; increasing covalency for higher charged species may also result in considerable metal/ligand/metal orbital mixing, rendering assignments based on localized descriptions less meaningful.

The reduction of the complexes leading to an EPR spectroscopically established  $(\text{dih-R}^{\bullet-})(\text{Ru}^{\text{II}})_2$  situation is accompanied by the expected disappearance of the LMCT band, the  $\text{Ru}^{\text{III}}$  centers are no longer available as targets of such a transition. There is an intense broad band emerging

(21) Kaim, W.; Ernst, S.; Kasack, V. *J. Am. Chem. Soc.* **1990**, *112*, 173.

(22) Cuss, M. E.; Gordon, N. R.; Pierpont, C. G. *Inorg. Chem.* **1986**, *25*, 3962.

(23) Moscherosch, M.; Waldhör, E.; Binder, H.; Kaim, W.; Fiedler, J. *Inorg. Chem.* **1995**, *34*, 4326.

(24) Ye, S.; Sarkar, B.; Liessner, F.; Schleid, Th.; van Slageren, J.; Fiedler, J.; Kaim, W. *Angew. Chem.* **2005**, *117*, 2140; *Angew. Chem., Int. Ed.* **2005**, *44*, 2103.

(25) Krejčík, M.; Danek, M.; Hartl, F. *J. Electroanal. Chem.* **1991**, *317*, 179.

(26) The resulting excited state can be formulated as involving an anion radical bridging two mixed-valent metal centers,  $\{(\mu\text{-dih-R}^{\bullet-})[\text{Ru}^{2.5-}(\text{acac})_2]_2\}$ . Related electronic structures were recently proposed for ground-state species (see ref 19).

**Table 3.** Redox Potentials<sup>a</sup> and Comproportionation Constants ( $K_c$ ) for the Complexes<sup>b</sup>

compound	couple				$K_c$ (+, -)
	I	II	III	IV	
$\{[(\text{acac})_2\text{Ru}]_2(\mu\text{-dih-Th})\}$ ( <b>1a</b> )	1.03(90)	0.27(90)	-0.94(70)	-1.69(100)	$10^{12.9}$ , $10^{12.8}$
$\{[(\text{acac})_2\text{Ru}]_2(\mu\text{-dih-Th})\}$ ( <b>1b</b> )	1.01(80)	0.25(70)	-0.96(80)	-1.68(80)	$10^{13.0}$ , $10^{12.2}$
$\{[(\text{acac})_2\text{Ru}]_2(\mu\text{-dih-Fu})\}$ ( <b>2</b> )	0.92(84)	0.16(63)	-1.03(80)	-1.81(80)	$10^{12.9}$ , $10^{13.2}$
$\{[(\text{acac})_2\text{Ru}]_2(\mu\text{-dih-Ph})\}$ ( <b>3a</b> )	0.90(80)	0.13(85)	-1.10(100)	-1.88(120)	$10^{13.0}$ , $10^{13.2}$
$\{[(\text{acac})_2\text{Ru}]_2(\mu\text{-dih-Ph})\}$ ( <b>3b</b> )	0.90(80)	0.12(90)	-1.13(90)	-1.87(170)	$10^{13.3}$ , $10^{12.6}$

<sup>a</sup> Potentials  $E^{\circ}_{298}/V$  ( $\Delta E/\text{mV}$ ) versus SCE. <sup>b</sup> In  $\text{CH}_3\text{CN}/0.1 \text{ M Et}_4\text{NClO}_4$

**Table 4.** EPR Data for Oxidized and Reduced Complexes<sup>a</sup>

compound <sup>a</sup>	$g_1$	$g_2$	$g_3$	$\Delta g^b$	$g_{\text{iso}}^c$
<b>1a</b> <sup>+</sup>	2.261	2.140	1.851	0.410	2.091
<b>1a</b> <sup>-</sup>	1.975	1.975	1.975	—	1.975
<b>1b</b> <sup>+</sup>	2.223	2.136	1.841	0.382	2.073
<b>1b</b> <sup>-</sup>	1.968	1.968	1.968	—	1.968
<b>2</b> <sup>+</sup>	2.236	2.115	1.844	0.392	2.072
<b>2</b> <sup>-</sup>	1.968	1.968	1.968	—	1.968
<b>3a</b> <sup>+</sup>	2.249	2.132	1.838	0.411	2.080
<b>3a</b> <sup>-</sup>	1.966	1.966	1.966	—	1.966
<b>3b</b> <sup>+</sup>	2.231	2.134	1.836	0.396	2.074
<b>3b</b> <sup>-</sup>	1.968	1.968	1.968	—	1.968

<sup>a</sup> Measurements in  $\text{CH}_3\text{CN}/0.1 \text{ M Bu}_4\text{NPF}_6$  at 110 K. <sup>b</sup>  $\Delta g = g_1 - g_3$ .

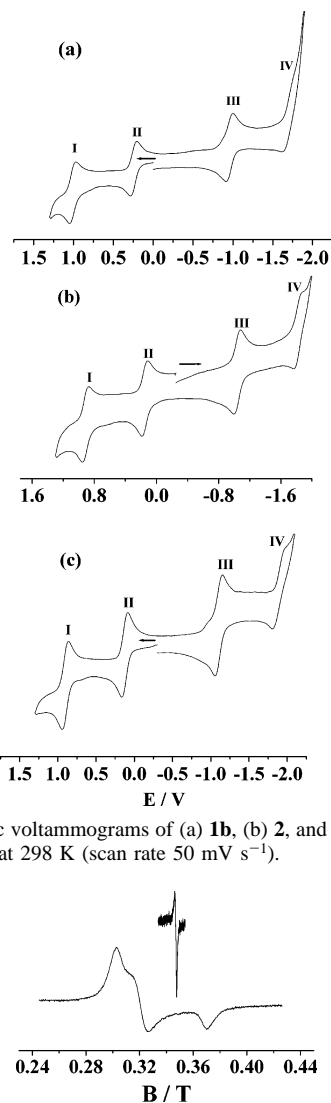
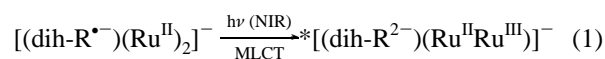
<sup>c</sup>  $g_{\text{iso}} = \sqrt{(g_1^2 + g_2^2 + g_3^2)/3}$ .

**Table 5.** Absorption Maxima  $\lambda_{\text{max}}$  (nm)<sup>a</sup> of Diruthenium Complexes  $[(\text{acac})_2\text{Ru}(\text{dih-R})\text{Ru}(\text{acac})_2]^n$  with Ring-Opened Tetrazines

N	<b>1a</b>	<b>1b</b>	<b>2</b>	<b>3a</b>	<b>3b</b>
0	734 (15.8) 350 (14.3) 270 (31.4)	718 (16.3) 353 (13.1) 268 (25.8)	744 (15.2) 347 (13.1) 273 (33.2)	729 (14.8) 352 (12.1) 270 (28.4)	716 (16.2) 353 (13.7) 267 (30.5)
	240 sh 240 sh	242 sh 242 sh	242 sh 242 sh	237 sh 237 sh	241 sh 241 sh
+	745 (10.3) 565 (4.9) 448 sh 292 sh 267 (30.2)	737 (11.2) 572 (5.2) 443 sh 293 sh 268 (26.8)	757 (9.3) 570 (5.0) 445 sh 272 (29.8)	718 (10.3) 545 sh 427 (4.2) 268 (24.5) 239 (23.9)	716 (12.2) 558 sh 430 sh 269 (28.4) 239 (27.0)
	241 sh 241 sh	243 sh 242 (24.9)	243 sh 1415 (9.3)	240 (26.8)	265 (26.7)
2+	803 (19.6) 268 (29.4) 242 sh	815 (18.9) 295 sh 268 (26.3)	800 (14.4) 278 (29.2)	794 (21.8) 292 sh 240 (26.8)	800 (22.5) 294 sh 265 (26.7)
		242 (24.9)			241 (28.2)
-	1423 (7.2) 660 (4.2)	1385 (8.0) 643 (4.1)	615 (4.3)	1390 (9.2) 590 (4.2)	1368 (9.4) 595 sh
	430 (11.1) 269 (32.5) 242 sh	428 (12.0) 268 (28.7) 241 sh	412 (9.5) 271 (30.9) 236 sh	436 (11.8) 269 (29.1) 236 sh	434 (12.9) 285 sh 269 (31.1) 239 (25.4)
2-	dec <sup>b</sup>	dec <sup>b</sup>	710 sh 531 (9.9) 466 (9.8) 272 (33.5) 238 sh	685 sh 492 (12.4) 269 (30.8) 285 sh 239 (24.6)	675 sh 494 (15.1) 268 (33.0) 287 sh 241 (28.1)

<sup>a</sup> From OTTLE spectroelectrochemistry in  $\text{CH}_3\text{CN}/0.1 \text{ M Bu}_4\text{NPF}_6$ ; molar extinction coefficients in  $10^3 \text{ M}^{-1} \text{ cm}^{-1}$  (in parentheses). <sup>b</sup> Partial decomposition on the time scale of the experiment (1 min).

in the near-infrared region around 1400 nm which, at first sight, could be attributed to the intervalence charge transfer (IVCT) transition of a mixed-valent situation  $(\text{dih-R}^{2-})\text{Ru}^{\text{II}}\text{-Ru}^{\text{III}}$ . However, since the EPR results unequivocally indicate the  $(\text{dih-R}^{\bullet-})(\text{Ru}^{\text{II}})_2$  formulation to be correct, that NIR band must be assigned otherwise, most likely to an MLCT transition from the electron-rich  $\text{Ru}^{\text{II}}$  centers to the  $\pi$ -accepting (i.e., reducible) radical bridge. In other words, the mixed-valent configuration is the close-lying excited state of that anionic form according to eq 1.

**Figure 5.** Cyclic voltammograms of (a) **1b**, (b) **2**, and (c) **3a** in  $\text{CH}_3\text{CN}/0.1 \text{ M Et}_4\text{NClO}_4$  at 298 K (scan rate  $50 \text{ mV s}^{-1}$ ).**Figure 6.** EPR Spectra of **1a**<sup>-</sup> (top) and **1a**<sup>+</sup> (bottom) in  $\text{CH}_3\text{CN}/0.1 \text{ M Bu}_4\text{NPF}_6$  at 110 K.

This assignment is supported by the correspondence between the absorption energy at about 0.88 eV and the potential differences of ca. 0.75 V between redox couple III and IV (Table 3).

Similar intense NIR bands at around 1600 nm have been reported for the related paramagnetic complexes  $\{(\mu\text{-adc-R})[\text{Ru}(\text{bpy})_2]_2\}^{3+}$ ,<sup>9</sup> however, there the EPR analysis of the well-detectable  $g$  anisotropy revealed sizable, substituent-dependent contributions from the metals according to a continuum between situations  $(\mu\text{-L}^{\bullet-})(\text{Ru}^{\text{II}})_2$  and  $(\mu\text{-L}^{2-})\text{Ru}^{\text{II}}\text{-Ru}^{\text{III}}$ .<sup>9</sup> It is thus important to note that NIR bands alone cannot be taken per se as unambiguous evidence for a mixed-



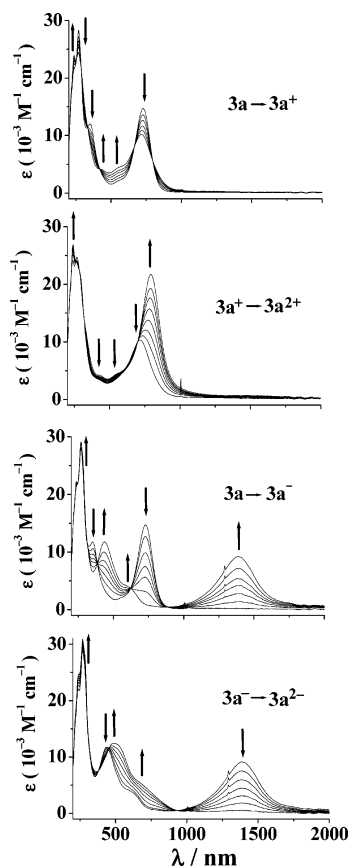


**Figure 7.** OTTLE spectroelectrochemistry of  $3a^n$  in  $\text{CH}_3\text{CN}/0.1 \text{ M Bu}_4\text{NPF}_6$ .

valence situation in metal complexes, especially in the presence of non-innocent ligands.

The difference between the partially mixed-valent complexes  $\{(\mu\text{-adc-R})[\text{Ru}(\text{bpy})_2]_2\}^{3+}$  and the closely related  $\{(\mu\text{-dih-R})[\text{Ru}(\text{acac})_2]_2\}^-$ , which are diruthenium(II) radical compounds, cannot be attributed to the ancillary ligands because  $\text{acac}^-$  favors the ruthenium(III) state<sup>15,16</sup> whereas  $\text{bpy}$  stabilizes ruthenium(II).<sup>27</sup> The origin of this difference lies rather in the bridging ligand situation where imine-containing compounds are easier to oxidize (and harder to reduce) than the carbonyl analogues. This effect, commonly explained via the higher electronegativity of O versus N, facilitates the oxidation of  $\text{dih-R}^{2-}$  to the radical anion  $\text{dih-R}^{\bullet-}$ , with concomitant results for the metal oxidation states.

Nevertheless, the spectral similarity between individual states  $\{(\mu\text{-dih-R})[\text{Ru}(\text{acac})_2]_2\}^n$  and corresponding complexes  $\{(\mu\text{-adc-R})[\text{Ru}(\text{bpy})_2]_2\}^{n+4}$  (cf. Scheme 6) does not only concern the paramagnetic intermediates ( $n = -1$ ) with their intense NIR bands or the oxidized forms ( $n = 0$ ) with very intense charge-transfer bands around 800 nm in both cases (Table 5),<sup>9</sup> it also extends to the reduced forms ( $n = -2$ ) which do not exhibit prominent bands at such long wavelengths because the bridging ligand and the metals exist in their reduced forms. The observed bands in the visible region are attributed to MLCT transitions directed at the acetylacetonate co-ligands.<sup>15,16,27</sup> The correspondence between the

structurally and electronically related redox systems  $\{(\mu\text{-dih-R})[\text{Ru}(\text{acac})_2]_2\}^n$  and  $\{(\mu\text{-adc-R})[\text{Ru}(\text{bpy})_2]_2\}^{n+4}$  is illustrated in Scheme 6. In addition to the correlation between the central two-step redox systems, the diacylhydrazido-bridged compounds can undergo further reduction at the 2,2'-bipyridine co-ligands while the donor effect of the  $\text{acac}^-$  ligands allows for further oxidation of  $(\mu\text{-dih-R})[\text{Ru}(\text{acac})_2]_2$ .

## Conclusion

In this work, we have shown that the 1,2,4,5-tetrazines cannot only be used as unusual ligands<sup>3</sup> with an intact six-membered heterocyclic ring in the strongly  $\pi$ -accepting and valence-exchange mediating<sup>28</sup> neutral form or in partially reduced (radical anion<sup>29</sup> or 1,4-dihydro<sup>30</sup>) states but that the products from reductive ring-opening after four-electron addition are also highly attractive new non-innocent bridging ligands. The form identified via structure determination of two compounds  $(\mu\text{-dih-R})[\text{Ru}(\text{acac})_2]_2$  is best described as 1,2-diiminohydrazido(2-) ( $\mu\text{-dih-R}^{2-}$ ) which can coordinate two metal centers to form a compact structure with edge-sharing unsaturated five-membered chelate rings and thus rather short metal-metal distances of about 4.8 Å. These structural and electronic effects also favor strong antiferromagnetic spin-spin interaction, as observed for the diruthenium(III) compounds  $(\mu\text{-dih-R})[\text{Ru}(\text{acac})_2]_2$ . The unsaturated ligand system is oxidized to a radical anion in diruthenium(II) complexes  $\{(\mu\text{-dih-R})[\text{Ru}(\text{acac})_2]_2\}^-$ , which exhibit intense bands in the near-infrared yet are *not* mixed-valent species according to comparative<sup>9,31</sup> EPR spectroscopy.

In contrast to previous recent reports<sup>5-7</sup> on complexes with ring-opened tetrazines (Scheme 1), the reaction presented here does not require coordinative support through substituents. Instead, all four nitrogen atoms from the former tetrazine ring are involved in bis-chelation of two metal centers. As a perspective, it may be envisaged that other electron-rich metal compounds can induce the ring-opening of tetrazines, either simple tetrazines such as phtz, non-chelating functional tetrazines such as bridging 3,6-bis(4,4'-pyridyl)-1,2,4,5-tetrazine,<sup>32</sup> or chelating tetrazine derivatives such as bptz.<sup>3</sup>

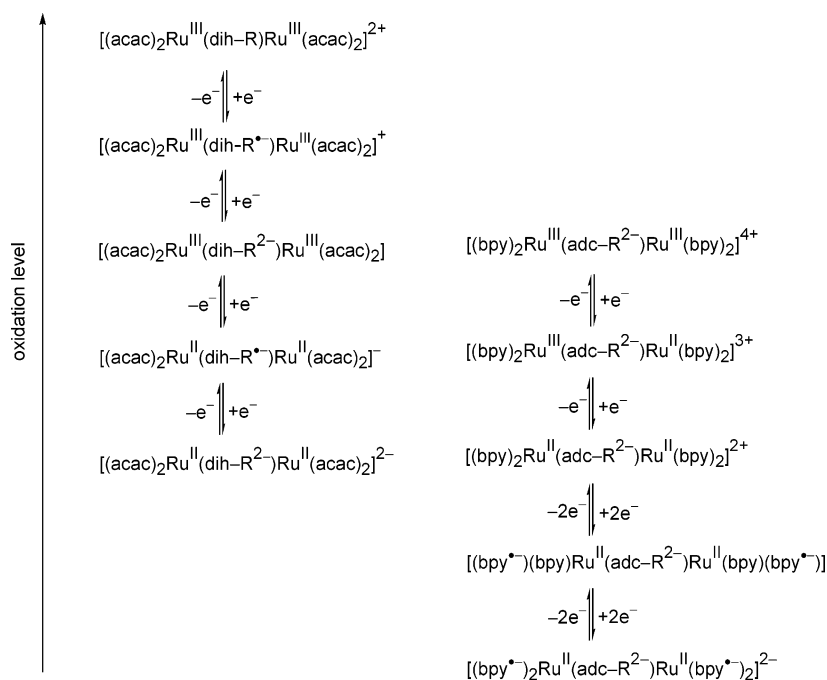
## Experimental Section

**General.** The precursor complex  $\text{Ru}(\text{acac})_2(\text{CH}_3\text{CN})_2$ <sup>33</sup> and the tetrazine-based ligands 3,6-bis(2-thienyl)-1,2,4,5-tetrazine (bttz),<sup>11</sup> 3,6-bis(2-furyl)-1,2,4,5-tetrazine (bftz),<sup>4</sup> and 3,6-diphenyl-1,2,4,5-

(27) Patra, S.; Sarkar, B.; Maji, S.; Fiedler, J.; Urbanos, F. A.; Jimenez-Aparicio, R.; Kaim, W.; Lahiri, G. K. *Chem. Eur. J.*, in press.

(28) (a) Poppe, J.; Moscherosch, M.; Kaim, W. *Inorg. Chem.* **1993**, 32, 2640. (b) Glöckle, M.; Kaim, W.; Klein, A.; Roduner, E.; Hübner, G.; Zalis, S.; van Slageren, J.; Renz, F.; Gütlich, P. *Inorg. Chem.* **2001**, 40, 2256.  
(29) Schwach, M.; Hausen, H.-D.; Kaim, W. *Inorg. Chem.* **1999**, 38, 2242.  
(30) Glöckle, M.; Hübner, K.; Kümmerer, H.-J.; Denninger, G.; Kaim, W. *Inorg. Chem.* **2001**, 40, 2263.  
(31) Remenyi, C.; Kaupp, M. *J. Am. Chem. Soc.* **2005**, 127, 11399.  
(32) (a) Kaim, W.; Kohlmann, S. *Inorg. Chem.* **1990**, 29, 1898. (b) Waldhör, E.; Zulu, M. M.; Zalis, S.; Kaim, W. *J. Chem. Soc., Perkin Trans. 2* **1996**, 1197. (c) Dinolfo, P. H.; Williams, M. E.; Stern, C. L.; Hupp, J. T. *J. Am. Chem. Soc.* **2004**, 126, 12989.  
(33) Kobayashi, T.; Nishina, Y.; Shimizu, K. G.; Satō, G. P. *Chem. Lett.* **1988**, 1137.

Scheme 6



tetrazine (phtz)<sup>34</sup> were prepared according to reported procedures. Other chemicals and solvents were reagent grade and used as received. For spectroscopic and electrochemical studies, HPLC grade solvents were used.

UV-vis-NIR spectroelectrochemical studies were performed in CH<sub>2</sub>CN/0.1 M Bu<sub>4</sub>NPF<sub>6</sub> at 298 K using an OTTLE cell<sup>25</sup> coupled with a J&M TIDAS spectrophotometer. Solution electrical conductivity was checked using a Systronic 305 conductivity bridge. Magnetic susceptibility was investigated with a PAR vibrating sample magnetometer. All neutral samples were found to be diamagnetic. <sup>1</sup>H NMR spectra were obtained with a 300 MHz Varian FT spectrometer. The EPR measurements were made in a two-electrode capillary tube<sup>21</sup> with a X-band Bruker system ESP300 equipped with a Bruker ER035M gaussmeter and a HP 5350B microwave counter. Cyclic voltammetric, differential pulse voltammetric, and coulometric measurements were carried out using a PAR model 273A electrochemistry system. Platinum wire working and auxiliary electrodes and an aqueous saturated calomel reference electrode (SCE) were used in a three-electrode configuration. The supporting electrolyte was Et<sub>4</sub>NClO<sub>4</sub>, and the solute concentration was ~10<sup>-3</sup> M. The half-wave potential  $E_{298}^{\circ}$  was set equal to 0.5- ( $E_{\text{pa}} + E_{\text{pc}}$ ), where  $E_{\text{pa}}$  and  $E_{\text{pc}}$  are anodic and cathodic cyclic voltammetric peak potentials, respectively. A platinum wire-gauze working electrode was used in coulometric experiments. All measurements were carried out under a dinitrogen atmosphere. The elemental analyses were carried out with a Perkin-Elmer 240C elemental analyzer. Electrospray mass spectra were recorded on a Micromass Q-ToF mass spectrometer.

**Synthesis of {Ru(acac)<sub>2</sub>}<sub>2</sub>(μ-dih-Th) (1a and 1b).** The precursor complex Ru(acac)<sub>2</sub>(CH<sub>3</sub>CN)<sub>2</sub> (100 mg, 0.26 mmol) and the ligand bttz (30 mg, 0.12 mmol) were dissolved in 20 mL of ethanol and the mixture was heated to reflux for 24 h under aerobic conditions. The initial orange color of the solution gradually changed to dark green, and the solvent of the reaction mixture was evaporated to

dryness under reduced pressure. The green solid thus obtained was dissolved in the minimum volume of CH<sub>2</sub>Cl<sub>2</sub> and purified by using a silica gel column. Initially, a red compound corresponding to Ru-(acac)<sub>3</sub> was eluted with CH<sub>2</sub>Cl<sub>2</sub>-CH<sub>3</sub>CN (20:1). With CH<sub>2</sub>Cl<sub>2</sub>-CH<sub>3</sub>CN (3:1), a green zone corresponding to a mixture of isomers **1a** (rac) and **1b** (meso) was eluted. The isomers were separated on a silica gel preparatory TLC plate using CH<sub>2</sub>Cl<sub>2</sub>-CH<sub>3</sub>CN (6:1). For **1a**: Yield = 15 mg (13.5%); Anal. Calcd for C<sub>30</sub>H<sub>36</sub>N<sub>4</sub>S<sub>2</sub>O<sub>8</sub>-Ru<sub>2</sub>: C, 42.45; H, 4.28; N 6.61. Found: C, 42.71; H, 4.12; N 6.39. ESI MS (CH<sub>2</sub>Cl<sub>2</sub>):  $m/z$  = 848.05 [M<sup>+</sup>] (calcd  $m/z$ , 848.00). <sup>1</sup>H NMR {(CD<sub>3</sub>)<sub>2</sub>SO}, δ (J/Hz): 12.08 (s, NH), 7.65 (d, 5.4), 7.50 (d, 3.6), 7.15 (t, 4.35, 4.35), 5.66 (s, CH(acac)), 4.91 (s, CH(acac)), 2.21 (s, CH<sub>3</sub>(acac)), 2.04 (s, CH<sub>3</sub>(acac)), 1.96 (s, CH<sub>3</sub>(acac)), 1.52 (s, CH<sub>3</sub>(acac)). For **1b**: Yield = 30 mg (27%); Anal. Calcd for C<sub>30</sub>H<sub>36</sub>N<sub>4</sub>S<sub>2</sub>O<sub>8</sub>Ru<sub>2</sub>: C, 42.45; H, 4.28; N 6.61. Found: C, 42.81; H, 4.63; N 6.97. ESI MS (CH<sub>2</sub>Cl<sub>2</sub>):  $m/z$  = 848.33 [M<sup>+</sup>] (calcd  $m/z$ , 848.00). <sup>1</sup>H NMR {(CD<sub>3</sub>)<sub>2</sub>SO}, δ (J/Hz): 12.13 (NH) 7.61 (d, 5.1), 7.16 (d, 3.0), 7.10 (t, 4.8, 3.6), 5.29 (s, CH(acac)), 5.11 (s, CH(acac)), 2.18 (s, CH<sub>3</sub>(acac)), 2.14 (s, CH<sub>3</sub>(acac)), 1.97 (s, CH<sub>3</sub>(acac)), 1.53 (s, CH<sub>3</sub>(acac)).

**Synthesis of {Ru(acac)<sub>2</sub>}<sub>2</sub>(μ-dih-Fu) (2).** The starting complex Ru(acac)<sub>2</sub>(CH<sub>3</sub>CN)<sub>2</sub> (100 mg, 0.26 mmol) and the ligand bftz (26 mg, 0.12 mmol) were taken in 20 mL of ethanol, and the mixture was heated to reflux for 4 h in air. The initial orange color of the solution gradually changed to dark green. The solvent of the reaction mixture was evaporated to dryness under reduced pressure, and the solid mass thus obtained was dissolved in the minimum volume of CH<sub>2</sub>Cl<sub>2</sub> to be purified by using a silica gel column. Initially, a red compound corresponding to Ru(acac)<sub>3</sub> was eluted with CH<sub>2</sub>-Cl<sub>2</sub>-CH<sub>3</sub>CN (50:1). With CH<sub>2</sub>Cl<sub>2</sub>-CH<sub>3</sub>CN (12:1), a green compound corresponding to **2** was separated later on. Yield = 35 mg (33%). Anal. Calcd for C<sub>30</sub>H<sub>36</sub>N<sub>4</sub>O<sub>10</sub>Ru<sub>2</sub> (816.06): C, 44.11; H, 4.45; N 6.86. Found: C, 44.52; H, 4.52; N, 6.98. ESI MS (CH<sub>2</sub>-Cl<sub>2</sub>):  $m/z$  = 816.06 [M<sup>+</sup>] (calcd  $m/z$ , 816.06). <sup>1</sup>H NMR data {(CD<sub>3</sub>)<sub>2</sub>SO}, δ (J/Hz): 12.15 (s, NH) 7.77 (d, 1.5), 7.10 (d, 4.5), 6.67 (t, 2.7, 2.7), 5.68 (s, CH(acac)), 5.00 (s, CH(acac)), 2.19 (s, CH<sub>3</sub>(acac)), 2.06 (s, CH<sub>3</sub>(acac)), 1.99 (s, CH<sub>3</sub>(acac)), 1.72 (s, CH<sub>3</sub>(acac)).

(34) (a) Abdel-Rahman, M. O.; Kire, M. A.; Tolba, M. N. *Tetrahedron Lett.* **1968**, 35, 3871. (b) Fischer, H.; Müller, Umminger, I.; Neugebauer, F. A. *J. Chem. Soc., Perkin Trans. II* **1988**, 413.

**Synthesis of {Ru(acac)<sub>2</sub>}<sub>2</sub>( $\mu$ -dih-Ph) (**3a** and **3b**).** A mixture of Ru(acac)<sub>2</sub>(CH<sub>3</sub>CN)<sub>2</sub> (100 mg, 0.26 mmol) and phtz (28 mg, 0.12 mmol) in 20 mL of ethanol was heated to reflux for 5 h under aerobic conditions. The initial orange color of the solution gradually changed to dark green, and the solvent of the reaction mixture was evaporated to dryness under reduced pressure. The green solid was dissolved in the minimum volume of CH<sub>2</sub>Cl<sub>2</sub> and purified using a silica gel column. Initially, red Ru(acac)<sub>3</sub> was eluted with CH<sub>2</sub>Cl<sub>2</sub>–CH<sub>3</sub>CN (15:1). With CH<sub>2</sub>Cl<sub>2</sub>–CH<sub>3</sub>CN (3:1), a mixture of isomers **3a** and **3b** was eluted. **3a** and **3b** were separated on a silica gel preparatory TLC plate using CH<sub>2</sub>Cl<sub>2</sub>–CH<sub>3</sub>CN (7:1). For **3a**: Yield = 25 mg (23%). Anal. Calcd for C<sub>34</sub>H<sub>40</sub>N<sub>4</sub>O<sub>8</sub>Ru<sub>2</sub>: C, 48.92; H, 4.83; N, 6.71. Found: C, 49.13; H, 4.91; N, 7.12. ESI MS (CH<sub>2</sub>Cl<sub>2</sub>): *m/z* = 836.24 [M<sup>+</sup>] (calcd *m/z*, 836.09). <sup>1</sup>H NMR, {(CD<sub>3</sub>)<sub>2</sub>SO},  $\delta$  (J/Hz): 12.15 (s, NH), 7.68 (multiplet for 2 phenyl ring protons), 7.40 (multiplet for 3 phenyl ring protons), 5.47 (s, CH(acac)), 4.81 (s, CH(acac)), 2.10 (s, CH<sub>3</sub>(acac)), 1.92 (s, 2CH<sub>3</sub>(acac)), 1.26 (s, CH<sub>3</sub>(acac)). For **3b**: Yield = 30 mg (27%). Anal. Calcd for C<sub>34</sub>H<sub>40</sub>N<sub>4</sub>O<sub>8</sub>Ru<sub>2</sub>: C, 48.92; H, 4.83; N, 6.71. Found: C, 49.25; H, 4.89; N, 6.99. ESI MS (CH<sub>2</sub>Cl<sub>2</sub>): *m/z* = 836.28 [M<sup>+</sup>] (calcd *m/z*, 836.09). <sup>1</sup>H NMR, {(CD<sub>3</sub>)<sub>2</sub>SO},  $\delta$  (J/Hz): 12.16 (s, NH) 7.40 (multiplet for 5 phenyl ring protons), 5.35 (s, CH(acac)), 5.09 (s, CH(acac)), 2.16 (s, CH<sub>3</sub>(acac)), 2.08 (s, CH<sub>3</sub>(acac)), 1.98 (s, CH<sub>3</sub>(acac)), 1.32 (s, CH<sub>3</sub>(acac)).

**X-ray Structure Determination.** Single crystals of **1b** and **3b** were grown by slow diffusion of a dichloromethane solution into *n*-hexane, followed by slow evaporation (**1b**) or by slow evaporation of a dimethyl sulfoxide solution (**3b**). The crystal of **1b** contains 2  $\times$  (0.25 H<sub>2</sub>O) molecules as solvent of crystallization. X-ray data of **1b** and **3b** were collected using Bruker SMART APEX CCD and Enraf-Nonius CAD-4 (MACH-3) single-crystal X-ray diffractometers, respectively. The structures of **1b** and **3b** were solved

and refined by full-matrix least-squares techniques on *F*<sup>2</sup> using SHELX-97 (SHELXTL program package) and SHELX-97, respectively.<sup>35</sup> The absorption corrections for **1b** and **3b** were done by SADABS and psi-scan, respectively, and all data were corrected for Lorentz and polarization effects. Hydrogen atoms were included in the refinement process as per the riding model.

One of the thiophene rings in the crystal of **1b** is disordered due to 180° rotation about the C16–C17 single bond so that the S2 and C18 atoms interchange their positions. Thus, the structure was refined considering the coincidence of S2' with C18 and C18' with S2. This model led to a very good convergence. Except for the disordered atoms of thiophene ring which were refined isotropically, all other non-hydrogen atoms were refined anisotropically.

**Acknowledgment.** Financial support received from the Department of Science and Technology, New Delhi (India), from the DAAD and the DFG (Germany) is gratefully acknowledged. X-ray structural studies for **3b** were carried out at the National Single Crystal Diffractometer Facility, Indian Institute of Technology, Bombay. Special acknowledgment is made to the Sophisticated Analytical Instrument Facility (SAIF), Indian Institute of Technology, Bombay, for providing facilities for NMR measurements.

**Supporting Information Available:** X-ray crystallographic file in CIF format for compounds **1b** and **3b**. This material is available free of charge via the Internet at <http://pubs.acs.org>.

IC051532P

(35) Sheldrick, G. M. *SHELX-97 program for crystal structure solution and refinement*; University of Göttingen: Göttingen, Germany, 1997.